Quasielastic knockout of alpha clusters by intermediate energy protons: Signatures of virtually excited states

Alexander A. Sakharuk[1] and Vladimir Zelevinsky[2,3]

[1]*Brest State University, Brest 224665, Belarus*

[2]*Department of Physics and Astronomy and National Superconducting Cyclotron Laboratory, Michigan State University, East Lansing, Michigan 48824*

[3]*Budker Institute of Nuclear Physics, Novosibirsk 630090, Russia*

The long-standing problem of experimental signatures for clustering effects in light nuclei is discussed for the conditions corresponding to a recent experiment. The specific reaction $^{12}C(p,p'\alpha)^8Be$ at incident proton energy 300 MeV and fixed proton and alpha-particle angles near the quasielastic peak is discussed. The Glauber approximation with a simple parametrization of the elementary nucleon-nucleon amplitude is used for calculating the cross section. The main emphasis is on the existence of virtually excited cluster configurations and their manifestation in experimental observables. The shell model wave function of the ^{12}C ground state is used to extract the weights of excited cluster components and to calculate their contributions to the cross section. The presence of several excited components and their complicated interference influence the shape and the height of the quasielastic peak; the change can reach an order of magnitude. It is shown that the cross section for cluster emission with the excitation of ^8Be into the first excited 2^+ state is small as compared to the process leaving ^8Be in its ground state. [S0556-2813(97)02701-5]

I. INTRODUCTION

Experimental studies of quasielastic cluster knockout reactions using coincidence methods have been conducted since the 1960's [1–3]. Such investigations are usually motivated by the following considerations.

At sufficiently high energies the experimental data reveal a direct reaction mechanism in which the incident particle interacts mainly with the knocked out cluster and the residual nucleus is simply a spectator. Thus it is hoped that from such investigations it is possible to extract information about spectroscopic factors of clusters in nuclei. The spectroscopic factor is simply the probability of finding the cluster inside the nucleus.

Along with the spectroscopic information, it is possible to deduce the momentum distribution of the knocked out cluster in the target nucleus, due to the relative simplicity of the reaction mechanism.

The last statement assumes that the theoretical interpretation of the experimental data allows us to separate effects of the reaction mechanism and nuclear structure on the cross section.

In the early stages the experimental data were analyzed in the framework of the plane-wave impulse approximation (PWIA) [4]. This very simple but efficient approach permits us to single out the "structure" factor in the triple knockout cross section. This factor can be calculated with one of the standard nuclear models. For the light nuclei it is natural to employ different variants of the shell-model description. As early as 1960, Balashov, Boyarkina, and Rotter predicted the α-particle momentum distributions in ^{12}C and ^{16}O nuclei, using the usual fractional parentage techniques [5]. At nearly the same time Beregi *et al.* [6] calculated the "effective numbers" of α clusters in various nuclei using fractional parentage coefficients (fpc's) in the translationally invariant shell model (TISM). Nevertheless, direct comparisons of the theoretical predictions with experimental data revealed the inadequacy of the PWIA scheme even at rather high energies (the most impressive test was made in [7]). Therefore in most cases the experimental data have been analyzed in the framework of the distorted-wave impulse approximation (DWIA) [8,9].

There is no doubt that the DWIA method as a subsidiary tool for the classification and ordering of experimental knock out data is more appropriate than the PWIA [7,10–13]. It also possesses predictive power and may be used as a guidepost in designing subsequent experiments. However the direct extraction of spectroscopic information and momentum distributions of knocked out clusters from experimental data even within the DWIA framework is not completely justified. The reasons for this conclusion are the following.

(1) There are several fairly severe approximations even in the most refined DWIA variants [9]. They relate mainly to obtaining a factorized form of the reaction cross section. The simple factorized form of the cross section used, as a rule, in extracting spectroscopic information from experimental data imposes strong restrictions on the states of the knocked out cluster inside the target nucleus. Almost all standard DWIA calculations are based on the assumption that the cluster is already preformed inside the target in its ground state. This is reasonable at relatively small projectile energies when the scattering of the incident particle off the cluster takes place in the surface region of the target. As the energy of the projectile increases, the probability of scattering by clusters deep inside the target nucleus increases too. There is no rea-

son to expect that a cluster knocked out from deep inside the target nucleus has the same internal state as a free cluster. The only justification for such an assumption is the desire to simplify the theoretical calculations.

(2) As a result of the quasielastic knockout reaction we have in the final state three or more interacting particles. Thus it is necessary to solve at least a three-body problem in order to correctly take into account the final-state interactions. The rigorous solution of the three-body problem is possible in principle, for example, in the framework of the Faddeev or K-harmonic approaches. But such a solution appears so complicated and cumbersome that the possibility of obtaining spectroscopic information from experimental data is questionable. Instead of the strict solution of the three-body problem, most versions of the DWIA use the so-called "pair approximation" replacing the true many-body interactions by pairwise interactions. Each pair of interactions may then be described in an optical-model approximation. However for some particular cases this approximation is hard to justify. For example, for the quasielastic knockout reaction $^{12}C(p,p'\alpha)^{8}Be$, the replacement of the true three-body strong interaction by three two-body strongly interacting subsystems (p-α, p-^{8}Be, and α-^{8}Be) seems questionable. As is known, ^{8}Be is a radioactive nucleus and has a very short lifetime, disintegrating into two α particles during a time comparable to characteristic reaction times. Thus a four-body final state results.

(3) The optical-model description of nuclear pairwise interactions in the initial and final states requires the knowledge of the corresponding optical potentials. They may be deduced from elastic scattering data for stable nuclei, but not for such systems as α-^{8}Be and p-^{8}Be. The only source for such potentials is DWIA calculations for different transfer reactions. For example, for the above-mentioned α-^{8}Be system one can consider the reaction $^{11}B(p,\alpha)^{8}Be$ and obtain the optical potential in the final state by fitting the experimental reaction cross sections. However such methods introduce additional uncertainties into the interpretation of knockout data.

Despite the limitations of the DWIA method, it remains the most flexible tool for interpretation of experimental knockout data. It is worthwhile to attempt to improve it, with a view to eliminating at least some shortcomings of this method. This paper pursues the goal of removing the restriction of the standard DWIA method to a definite choice of the state of the cluster in the target nucleus. At the same time the purpose of this work is to try to find signatures of the so-called "virtually excited" [14–16] clusters in relatively low-energy quasielastic knockout reactions.

As the first attempt of this kind, our approach lacks complete rigor. Until now the theoretical treatment of similar reactions was undertaken mostly at high energies of the incident proton and at very large momentum transfer [15,16]. Then it is natural to apply a relatively simple Glauber description [17] of the reaction mechanism. Moreover, in this case, contrary to the low-energy region, one may use the unique parametrization of the elementary nucleon-nucleon scattering amplitudes [18] significantly simplifying the consideration. A particular $^{12}C(p,p'\alpha)^{8}Be$ quasielastic knockout reaction was the most thoroughly analyzed in this way [15]. Unfortunately, up to now experimental investigations
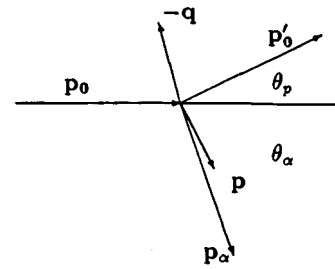

FIG. 1. Geometry of the experiment. The notations of the momenta are $\mathbf{p}_0$ (incident proton), $\mathbf{p}_0'$ (scattered proton), $\mathbf{p}_\alpha$ (emitted alpha particle), $-\mathbf{q}$ (recoil ^{8}Be nucleus), $\mathbf{p}=\mathbf{p}_0-\mathbf{p}_0'$ (proton momentum transfer); the angles θ_p and θ_α correspond to the directions of the final proton and alpha particle, respectively.

of this and other quasielastic knockout reactions at high energies have not been carried out. Recently measurements with polarized protons at comparatively low incident energy, $E_p=296$ MeV, on the targets ^{6}Li, ^{7}Li, ^{9}Be, and ^{12}C, and at different proton scattering angles, $\theta_p=35°$, $45°$, and $55°$, were performed in Osaka [19]. The analysis of the results is under progress. The present work is an attempt to estimate the role of structure effects, including those of virtually excited clusters, for those experimental conditions. We limit ourselves to consideration of the reaction $^{12}C(p,p'\alpha)^{8}Be$.

II. DESCRIPTION OF THE FORMALISM

The formalism used for the description of quasielastic knockout reactions may be divided into parts relating to the nuclear structure and the reaction mechanism (as in the usual DWIA method). The nuclear structure part is the central point of this work, and we attempt to make as few approximations and restrictions as possible. All simplifications used will be carefully examined and discussed. For the reaction part we deliberately choose the Glauber eikonal approach [17] for description of the proton-α cluster interaction, with a view to simplify our calculations. The Glauber approximation in the real experimental situation is somewhat doubtful due to relatively small energy of the initial projectile, 296 MeV, and the large proton scattering angles, 35° and 45°. Nevertheless we hope that the results of our treatment will be reasonable, at least concerning the relative contribution of virtually excited clusters to the reaction cross section. In addition, it is possible to introduce a number of corrections [33,20–25] to the standard eikonal approximation, extending the bounds of its applicability.

A. Kinematics

We assume the kinematical conditions of the Osaka experiment. The initial proton beam energy is 296 MeV, the knockout cross section is measured in coincidence for two coplanar laboratory geometries: the emission angles for final proton and alpha cluster, respectively, are (i) $\theta_p=35°$ and $\theta_\alpha=65.75°$; (ii) $\theta_p=45°$ and $\theta_\alpha=59.83°$. The angles are fixed in all our calculations (the polar axis corresponds to the incident proton beam). The coincidence cross section was measured as a function of the scattered proton energy. Figure 1 shows the geometry of the experiment and defines the notations.
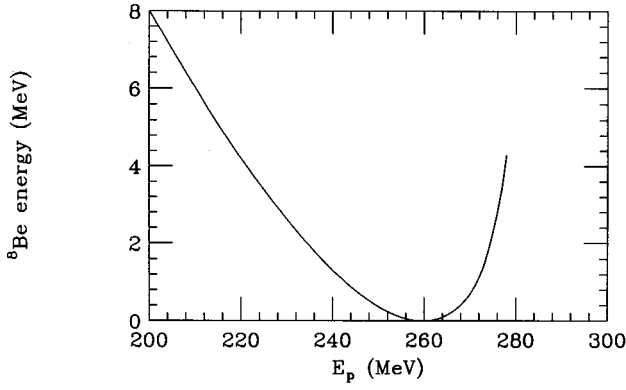
FIG. 2. Energy of the residual ^{8}Be nucleus vs energy of the scattered proton for $\theta_p = 35°$. The quasielastic peak corresponds to $E_p = 260$ MeV.

We use a fully relativistic kinematic description in the laboratory frame. This is quite necessary with respect to the incident and scattered proton, but less important for the α cluster and especially for the residual ^{8}Be nucleus, at least in the region of the quasielastic peak.

Energies of the emitted α cluster corresponding to different values of scattered proton kinetic energy E_p at $\theta_p = 35°$ vary almost linearly from 80 MeV at $E_p = 200$ MeV to zero at the kinematical boundary close to $E_p = 278$ MeV. In the region of our main interest, the quasielastic peak, the typical energies of α clusters range from 7 to 40 MeV. The energy of the residual ^{8}Be nucleus is shown in Fig. 2. The position of the quasielastic peak of the cross section is clearly seen as the point where the momentum of the residual nucleus is zero. This corresponds to the energy $E_p = 260$ MeV of the scattered proton. On the next picture (Fig. 3) one can see the angle of flight of the residual nucleus. It is interesting that at the point corresponding to the quasielastic peak, ~90°, this quantity changes irregularly.

B. Reaction mechanism

The triple cross section for the ^{12}C$(p,p'\alpha)^8$Be knockout reaction is computed in the usual way [26]:

$$\frac{d\sigma}{dE'd\Omega_p'd\Omega_\alpha} = \frac{m_p}{(2\pi)^2}\frac{p_\alpha E_\alpha p_0'E'}{p_0}\,|T_{fi}|^2. \quad (1)$$
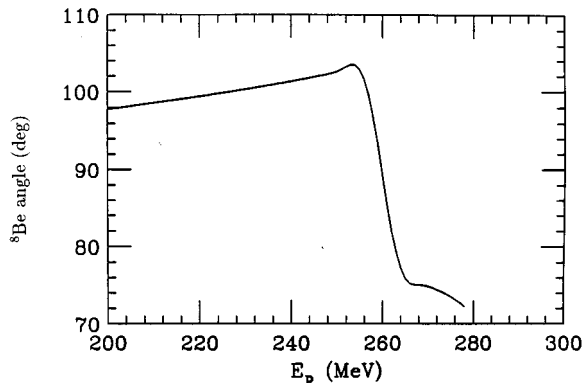

FIG. 3. The angle of the residual ^{8}Be nucleus vs energy of the scattered proton for $\theta_p = 35°$.

Here we introduce the following notations: $\mathbf{p}_\alpha$, $\mathbf{p}_0'$, and $\mathbf{p}_0$ are the momenta of the knocked out α cluster, scattered proton, and incident proton, respectively; E_α and E' are total energies of the α cluster and scattered proton ($E_\alpha = \sqrt{p_\alpha^2 + m_\alpha^2}$); m_p is the proton mass; and $T_{fi} = -(2\pi/m)g_{fi}$ is the transition amplitude where m is the proton-cluster reduced mass. The eikonal scattering amplitude is

$$g_{fi} = \frac{ip_0}{2\pi}\int d\boldsymbol{\rho}\,\exp(i\mathbf{p}\cdot\boldsymbol{\rho})\langle\Psi_f|\hat{\Omega}|\Psi_i\rangle. \quad (2)$$

Here $\mathbf{p} = \mathbf{p}_0 - \mathbf{p}_0'$ is the momentum transfer; $\boldsymbol{\rho}$ is the two-dimensional impact parameter vector in the plane perpendicular to the direction of proton motion; Ψ_i is the initial wave function of the target nucleus; and Ψ_f is the final wave function of the system $\alpha + ^8$Be.

The Glauber operator $\hat{\Omega}$

$$\hat{\Omega} = \sum_{j=1}^{4}\hat{\omega}_j - \sum_{1=j<k}^{4}\hat{\omega}_j\hat{\omega}_k + \sum_{1=j<k<l}^{4}\hat{\omega}_j\hat{\omega}_k\hat{\omega}_l - \prod_{j=1}^{4}\hat{\omega}_j \quad (3)$$

describes the scattering of the incident proton by the nucleons of the α cluster, for all possible multiplicities. In terms of the elementary scattering amplitude $f(\mathbf{p})$, corresponding to the scattering of the incident proton by the individual nucleons with the momentum transfer $\mathbf{p}$,

$$\hat{\omega}_j = \frac{1}{2\pi ip_0}\int f_j(\mathbf{p}_j)\exp[-i\mathbf{p}_j\cdot(\boldsymbol{\rho}-\boldsymbol{\rho}_j)]d\mathbf{p}_j. \quad (4)$$

For the sake of simplicity, we have omitted the formulas which take into account corrections [21,22] to the standard Glauber approach. But our actual calculations were made with these corrections.

C. The PWIA approximation

1. Initial wave function

Before using the DWIA scheme, let us examine the simpler PWIA approach. It gives the nice possibility to introduce the refined nuclear structure consideration without complications connected with the reaction mechanism.

The initial shell-model wave function of the target nucleus is taken in the intermediate coupling scheme

$$\Psi_i = \sum_{\{[f],L,S\}}a_{[f]LS}^{A,JT}|A[f]NLST:J,M_J,M_T\rangle. \quad (5)$$

Here $A = 12$ is the target mass number, $[f]$ is the Young scheme defining the spatial symmetry of the each component of the total wave function, N is the number of oscillator

quanta for a given configuration, and the total angular momentum $\mathbf{J}=\mathbf{L}+\mathbf{S}$. We have the following possible set of components $\{[f],L,S\}=\{([44]00),([431]11),([422]00),([422]22),([332]11)\}$ [27]. In the Young schemes only the p-shell parts are shown to avoid excessively complicated notations. In Table I one can see the main components of the wave function of the ^{12}C ground state along with their corresponding amplitudes.

Each component of Eq. (5) possesses good quantum numbers and may be presented as a superposition of products of the wave functions for the internal states of the cluster (b particles, N_0 oscillator quanta) and the residual nucleus ($A-b$ particles, N_1 quanta) and their relative motion with $n=N-N_0-N_1$ oscillator quanta and the relative orbital momentum Λ. Using the fractional parentage technique in the TISM [14] we obtain

$$|A[f]NLST:J,M_J,M_T\rangle = \sum \langle A\,\alpha[f]NLST|A-b[f_1]N_1L_1S_1T_1;n\Lambda,b[f_0]N_0L_0S_0T_0\{\mathcal{L}\}\rangle(-1)^{\Lambda+L_0+j+S_0}$$

$$\times \sqrt{(2J_1+1)(2j+1)(2L+1)(2S+1)(2\mathcal{L}+1)(2J_0+1)}$$

$$\times \begin{Bmatrix} L_1 & S_1 & J_1 \\ \mathcal{L} & S_0 & j \\ L & S & J \end{Bmatrix} \begin{Bmatrix} \Lambda & L_0 & \mathcal{L} \\ S_0 & j & J_0 \end{Bmatrix} \sum_{M_{T_1},M_{T_0}} (T_1M_{T_1},T_0M_{T_0}|TM_T)$$

$$\times \sum_{M_{L_0},M_{S_0},M_{J_0},M_\Lambda,m_j,M_{J_1}} (L_0M_{L_0},S_0M_{S_0}|J_0M_{J_0})(J_1M_{J_1},jm_j|JM_J)$$

$$\times (\Lambda M_\Lambda,J_0M_{J_0}|jm_j)|n\Lambda M_\Lambda\rangle|A-b[f_1]N_1L_1S_1T_1:J_1M_{J_1},M_{T_1}\rangle$$

$$\times |b[f_0]N_0L_0S_0T_0:M_{L_0}M_{S_0},M_{T_0}\rangle. \tag{6}$$

The first sum is taken over possible quantum numbers $[f_0]$, N_0,L_0,S_0,T_0,J_0 of the cluster, $[f_1],N_1,L_1,S_1,T_1,J_1$ of the residual nucleus, and the quantum numbers of relative motion n,Λ. We use the following scheme of isospin and angular momentum coupling: $\mathbf{T}_1+\mathbf{T}_0=\mathbf{T}$, $\mathbf{L}_0+\mathbf{S}_0=\mathbf{J}_0$, $\mathbf{\Lambda}+\mathbf{J}_0=\mathbf{j}$, $\mathbf{J}_1+\mathbf{j}=\mathbf{J}$. The first factor in Eq. (6) is the fpc in TISM, and the others are the usual Clebsch-Gordan coefficients, and $6j$ and $9j$ symbols which, together with all algebraic factors, appear as a result of conversion from the coupling scheme $\mathbf{T}_1+\mathbf{T}_0=\mathbf{T}$, $\mathbf{S}_1+\mathbf{S}_0=\mathbf{S}$, $\mathbf{\Lambda}+\mathbf{L}_0=\mathcal{L}$, $\mathbf{L}_1+\mathcal{L}=\mathbf{L}$, $\mathbf{L}+\mathbf{S}=\mathbf{J}$, for which the fpc in TISM are usually defined [14], to the one used above.

2. Final wave function

The final state wave function

$$\Psi_f^{(-)}=\hat{\mathcal{A}}[\exp(i\mathbf{p}_\alpha\cdot\mathbf{R}_\alpha)\exp(-i\mathbf{q}\cdot\mathbf{R}_{A-b})$$
$$\times \Psi_f^{A-b}|4[4]0000:000\rangle] \tag{7}$$

is the antisymmetrized product of the internal wave functions of the emitted α cluster $|b=4[4]0000:000\rangle$ and the residual ^{8}Be nucleus Ψ_f^{A-b}, and the plane waves corresponding to their free motion. The vector $\mathbf{q}$ defines the momentum distribution of the virtually excited α clusters in the ^{12}C target. For the internal wave function of the residual nucleus one can again use the shell-model wave function in the interme-

TABLE I. The components of the ^{12}C ground-state wave function.

$[f]$	L	S	$a^{12,00}_{[f]LS}$
[44]	0	0	0.84
[431]	1	1	0.492
[422]	0	0	0.064
[422]	2	2	−0.2
[332]	1	1	0.086

TABLE II. The components of the ^{8}Be ground-state wave function.

$[f_f]$	L_f	S_f	$a^{8,00}_{[f_f]L_fS_f}$
[4]	0	0	0.985
[31]	1	1	−0.171
[22]	0	0	−0.033
[22]	2	2	−0.019
[211]	1	1	0.011

diate coupling scheme. We consider here only the ground state $J^\pi = 0^+$ and the first excited state $J^\pi = 2^+$ of ^{8}Be with the excitation energy 2.9 MeV which might not be resolved in the real experiment. The amplitudes for these states,

$$\Psi_f^{A-b} = \sum_{\{[f_f]L_f S_f\}} a_{[f_f]L_f S_f}^{A-b,J_f T_f}$$

$$\times |A-b[f_f]N_f L_f S_f T_f : J_f, M_{J_f}, M_{T_f}\rangle, \qquad (8)$$

are shown in Tables II and III [27], for the ground and the first excited state, respectively.

The antisymmetrization operator $\hat{\mathcal{A}}$ may be removed due to the antisymmetry of the initial- and final-state wave func-

tions and symmetry of the interaction operator. It produces the usual combinatorial factor. The exponential factor in Eq. (7) may be rewritten as $\exp(-i\mathbf{p}_\alpha \cdot \mathbf{R}_\alpha)\exp(i\mathbf{q} \cdot \mathbf{R}_{A-b}) = \exp(-i\mathbf{p} \cdot \mathbf{R}_\alpha)\exp(i\mathbf{q} \cdot \mathbf{R})$, where $\mathbf{R} = \mathbf{R}_{A-b} - \mathbf{R}_\alpha$ is the relative coordinate of the residual nucleus and the knocked out α cluster.

3. Transition probability

Taking into account the explicit form for the relative motion wave function $|n\Lambda M_\Lambda\rangle = \varphi_{n\Lambda}(R)Y_{\Lambda M_\Lambda}(\hat{\mathbf{R}})$ and integrating over angles of the relative coordinate $\mathbf{R}$, we obtain for the eikonal scattering amplitude (2)

$$g_{fi} = \frac{ip_0}{2\pi} 4\pi \sum_{\{[f]L,S\}} a_{[f]LS}^{A,JT} \sum_{\{[f_f]L_f S_f\}} a_{[f_f]L_f S_f}^{A-b,J_f T_f} \times \sum \langle A\alpha[f]NLST|A-b\alpha_1[f_1]N_1 L_1 S_1 T_1 ; n\Lambda, b[f_0]N_0 L_0 S_0 T_0\{\mathcal{L}\}\rangle$$

$$\times (-1)^{\Lambda+L_0+j+S_0}\sqrt{(2J_1+1)(2j+1)(2L+1)(2S+1)(2\mathcal{L}+1)(2J_0+1)} \begin{Bmatrix} L_1 & S_1 & J_1 \\ \mathcal{L} & S_0 & j \\ L & S & J \end{Bmatrix}$$

$$\times \begin{Bmatrix} \Lambda & L_0 & \mathcal{L} \\ S_0 & j & J_0 \end{Bmatrix} \sum_{M_{T_1},M_{T_0}} (T_1 M_{T_1}, T_0 M_{T_0}|TM_T) i^\Lambda \sum_{M_{L_0},M_{S_0},M_{J_0},M_\Lambda,m_j,M_{J_1}} (L_0 M_{L_0}, S_0 M_{S_0}|J_0 M_{J_0})(J_1 M_{J_1},jm_j|JM_J)$$

$$\times (\Lambda M_\Lambda, J_0 M_{J_0}|jm_j) W_{n\Lambda} Y_{\Lambda M_\Lambda}(\hat{\mathbf{q}}) B_{fi}(p)\langle A-b[f_f]N_f L_f S_f T_f : J_f, M_{J_f}, M_{T_f}|A-b[f_1]N_1 L_1 S_1 T_1 : J_1 M_{J_1}, M_{T_1}\rangle.$$

$$(9)$$

Here

$$W_{n\Lambda} = \int_0^\infty R^2 j_\Lambda(qR)\varphi_{n\Lambda}(R)dR. \qquad (10)$$

We have also introduced the factor

$$B_{fi}(p) = \int d\boldsymbol{\rho} \exp[i\mathbf{p} \cdot (\boldsymbol{\rho} - \mathbf{R}_b)] \times \langle 4[4]0000:000|\hat{\Omega}|b[f_0]$$

$$\times N_0 L_0 S_0 T_0 : M_{L_0}M_{S_0},M_{T_0}\rangle \qquad (11)$$

TABLE III. The components of the 2^+ wave function in ^{8}Be.

$[f_f]$	L_f	S_f	$a_{[f_f]L_f S_f}^{8,00}$
[4]	2	0	0.985
[31]	1	1	0.096
[31]	2	1	−0.126
[31]	3	1	−0.063
[22]	0	2	0.01
[22]	2	0	0.013
[22]	2	2	0.015
[211]	1	1	0.009

that describes the scattering of the projectile on the α cluster with the possible transition of the cluster from the initial intrinsic state into the final state of the real emitted alpha particle. In the nondiagonal case (with respect to the state of the α cluster, $f \neq i$) we call this factor the deexcitation amplitude.

Assuming unpolarized protons and nuclei, the expression for the transition probability, the square of g_{fi} averaged over the projections of initial nuclei and summed over the projection of final nuclei, takes the form

$$\overline{|g_{fi}|^2} \propto \sum W_{n\Lambda}W_{n'\Lambda'}Y_{\Lambda M_\Lambda}(\hat{\mathbf{q}})[Y_{\Lambda' M_\Lambda}(\hat{\mathbf{q}})]^*$$

$$\times B_{fi}(p)[B_{fi'}(p)]^*. \qquad (12)$$

Here the $B_{fi'}(p)$ differs from the $B_{fi}(p)$ by the set of permissible cluster quantum numbers in the target nucleus. This complicated expression contains all effects of the interference between various virtual cluster states inside the target nucleus.

D. Deexcitation amplitudes

From the structure of the Glauber operator (3) we obtain an expansion of the deexcitation amplitudes in terms of the

scattering multiplicity

$$B_{fi}(p) = B_{fi}^{(1)} + B_{fi}^{(2)} + B_{fi}^{(3)} + B_{fi}^{(4)}. \qquad (13)$$

According to the experimental conditions, we consider in detail only the two lowest scattering multiplicities, since the higher-order terms exponentially decrease with the momentum transfer.

For the *first multiplicity* we have, after integrating over the two-dimensional vectors $\boldsymbol{\rho}$ and $\mathbf{p}_j$, the momentum transfer to the jth nucleon,

$$B_{fi}^{(1)} = \frac{(2\pi)^2}{2\pi i p_0} \left\langle f \left| \sum_{j=1}^{4} f_j(\mathbf{p}_j) \exp(i\mathbf{p}\cdot(\boldsymbol{\rho}_j - \mathbf{R}_b)) \right| i \right\rangle, \qquad (14)$$

where f and i refer to the final and initial cluster state, respectively. This matrix element is calculated with the use of the one-particle fractional parentage technique. Thus for the internal wave function we obtain the following expansion:

$$\begin{aligned}
|i\rangle &= |4[4]N_0 L_0 S_0 T_0 M_{L_0} M_{S_0} M_{T_0}\rangle \\
&= \sum_{N_2,L_2,S_2,T_2,n_2 l_2} \langle 4[4]N_0 L_0 S_0 T_0 | 3[3]N_2 L_2 S_2 T_2, n_2 l_2 \rangle \sum_{m_{t_2},M_{T_2}} \left(T_2 M_{T_2}, \frac{1}{2} m_{t_2} \middle| T_0 M_{T_0} \right) \\
&\quad \times \sum_{m_{s_2},M_{S_2}} \left(S_2 M_{S_2}, \frac{1}{2} m_{s_2} \middle| S_0 M_{S_0} \right) \sum_{m_{l_2},M_{L_2}} (L_2 M_{L_2}, l_2 m_{l_2} | L_0 M_{L_0}) | 3[3]N_2 L_2 S_2 T_2 M_{L_2} M_{S_2} M_{T_2} \rangle \\
&\quad \times \left| n_2 l_2 \frac{1}{2} \frac{1}{2} m_{l_2} m_{s_2} m_{t_2} \right\rangle.
\end{aligned} \qquad (15)$$

Here $\langle 4[4]N_0 L_0 S_0 T_0 | 3[3]N_2 L_2 S_2 T_2, n_2 l_2 \rangle$ is the one-particle fpc in the TISM, $|n_2 l_2 \frac{1}{2}\frac{1}{2}m_{l_2}m_{s_2}m_{t_2}\rangle$ is the wave function of the fourth nucleon, and $|3[3]N_2 L_2 S_2 T_2 M_{L_2} M_{S_2} M_{T_2}\rangle$ is the wave function of the three-nucleon system. As usual, it is necessary to transform to a new set of internal Jacobi coordinates $\{\mathbf{x}_j\}$ for the emitted cluster. The new coordinate for the bth nucleon is connected with the old one as

$$\boldsymbol{\rho}_b - \mathbf{R}_b = -\frac{b-1}{b}\mathbf{x}_{b-1}.$$

After routine computations one obtains the relatively simple expression for the $B^{(1)}$,

$$\begin{aligned}
B^{(1)} &= -i\frac{2\pi^{1/2}}{p_0} Y_{L_0 M_{L_0}}(\hat{\mathbf{p}})[f_{pp} + f_{pn}] \\
&\quad \times \left\langle 4[4]N_0 L_0 00 \middle| 3[3]00\frac{1}{2}\frac{1}{2}, N_0 L_0 \right\rangle \\
&\quad \times \left\langle 4[4]0000 \middle| 3[3]00\frac{1}{2}\frac{1}{2}, 00 \right\rangle I_{N_0 L_0}(3p/4),
\end{aligned} \qquad (16)$$

where the radial integral is defined by

$$I_{nl}(p) = 4\pi(-i)^l \int_0^\infty R_{00}(x) j_l(px) R_{nl}(x) x^2 dx. \qquad (17)$$

The first multiplicity transition is diagonal with respect to the spin-isospin cluster quantum numbers which are fixed by

the corresponding quantum numbers of the residual nucleus. For the lowest states of the rotational band 0^+, 2^+, 4^+ we have $T_{\mathrm{Be}}=0$.

The radial integrals (17) may be easily calculated analytically with the harmonic-oscillator wave functions. For the oscillator radius we use the value $r_0 = 1.38$ fm obtained from the electron scattering data on ^{4}He [28]. Note that it is necessary to recompute this value for the Jacobi coordinate of the fourth α cluster nucleon. Such recalculation gives the value 1.6 fm for the oscillator radius r_0. The magnitudes of the deexcitation amplitudes are very sensitive to this parameter and the choice of an incorrect value may significantly distort the results. The one-particle fpc in the TISM used in our calculations are computed in Appendix A.

For the *second multiplicity*, Eqs. (3) and (11) give

$$\begin{aligned}
B_{fi}^{(2)} &= \frac{-1}{(2\pi i p_0)^2} \left\langle f \left| \sum_{1=j<k}^{4} \int \exp[i\boldsymbol{\rho}\cdot(\mathbf{p} - \mathbf{p}_j - \mathbf{p}_k)]d\boldsymbol{\rho} \right. \right. \\
&\quad \times \int f_j(\mathbf{p}_j) f_k(\mathbf{p}_k) \exp(i\mathbf{p}_j\cdot\boldsymbol{\rho}_j + i\mathbf{p}_k\cdot\boldsymbol{\rho}_k \\
&\quad \left. \left. -i\mathbf{p}\cdot\mathbf{R}_b)d\mathbf{p}_j d\mathbf{p}_k \right| i \right\rangle \\
&= \frac{-(2\pi)^2}{(2\pi i p_0)^2} \left\langle f \left| \sum_{1=j<k}^{4} \int f_j(\mathbf{p}_j) f_k(\mathbf{p}_k) \exp(i\mathbf{p}_j\cdot\boldsymbol{\rho}_j \right. \right. \\
&\quad \left. \left. +i\mathbf{p}_k\cdot\boldsymbol{\rho}_k - i\mathbf{p}\cdot\mathbf{R}_b)\delta(\mathbf{p} - \mathbf{p}_j - \mathbf{p}_k)d\mathbf{p}_j d\mathbf{p}_k \right| i \right\rangle. \qquad (18)
\end{aligned}$$

In order to calculate the remaining integral one needs to make the change of variables $\mathbf{Q}_k = \mathbf{p}_k + \mathbf{p}_j$, $\mathbf{Q}_j = 1/2(\mathbf{p}_k - \mathbf{p}_j)$ with the Jacobian of this transition equal to 1. Here we ap-

Table IV. The two particle fpc in the TISM.

N_0	L_0	S_2	T_2	n_2	l_2	N_3	L_3	Coefficient	N_0	L_0	S_2	T_2	n_2	l_2	N_3	L_3	Coefficient
0	0	0	1	0	0	0	0	$\dfrac{-1}{\sqrt{2}}$	0	0	1	0	0	0	0	0	$\dfrac{1}{\sqrt{2}}$
2	0	0	1	2	0	0	0	$\dfrac{-1}{\sqrt{6}}$	2	0	1	0	2	0	0	0	$\dfrac{1}{\sqrt{6}}$
2	0	0	1	0	0	2	0	$\dfrac{-1}{\sqrt{6}}$	2	0	1	0	0	0	2	0	$\dfrac{1}{\sqrt{6}}$
2	2	0	1	2	2	0	0	$\dfrac{-1}{\sqrt{6}}$	2	2	1	0	2	2	0	0	$\dfrac{1}{\sqrt{6}}$
2	2	0	1	0	0	2	2	$\dfrac{-1}{\sqrt{6}}$	2	2	1	0	0	0	2	2	$\dfrac{1}{\sqrt{6}}$
4	0	0	1	4	0	0	0	$\dfrac{-1}{\sqrt{10}}$	4	0	1	0	4	0	0	0	$\dfrac{1}{\sqrt{10}}$
4	0	0	1	2	0	2	0	$\dfrac{-1}{3\sqrt{2}}$	4	0	1	0	2	0	2	0	$\dfrac{1}{3\sqrt{2}}$
4	0	0	1	2	2	2	2	$\dfrac{-2}{3\sqrt{15}}$	4	0	1	0	2	2	2	2	$\dfrac{2}{3\sqrt{15}}$
4	2	0	1	4	2	0	0	$\dfrac{\sqrt{7}}{3\sqrt{30}}$	4	2	1	0	4	2	0	0	$\dfrac{-\sqrt{7}}{3\sqrt{30}}$
4	2	0	1	2	2	2	0	$\dfrac{-1}{\sqrt{10}}$	4	2	1	0	2	2	2	0	$\dfrac{1}{\sqrt{10}}$
4	2	0	1	2	0	2	2	$\dfrac{\sqrt{7}}{3\sqrt{30}}$	4	2	1	0	2	0	2	2	$\dfrac{-\sqrt{7}}{3\sqrt{30}}$
4	4	0	1	4	4	0	0	$\dfrac{-1}{\sqrt{10}}$	4	4	1	0	4	4	0	0	$\dfrac{1}{\sqrt{10}}$
4	4	0	1	2	2	2	2	$\dfrac{1}{\sqrt{15}}$	4	4	1	0	2	2	2	2	$\dfrac{-1}{\sqrt{15}}$

proach the significant point connected with the important approximation used in standard Glauber calculations,

$$f_j\left(\frac{1}{2}\,\mathbf{p}\pm\mathbf{Q}_j\right)\simeq f_j\left(\frac{1}{2}\,\mathbf{p}\right).$$

This approximation assumes that the nucleon momenta inside the target nucleus are significantly less than the momentum transferred to the nucleons by the incident proton. In our case the momentum transfer as a function of E_p smoothly changes in a narrow region between 460 and 475 MeV/c. Thus the above assertion seems to be too optimistic and unsubstantiated. As we mentioned, this approximation can be easily improved using, instead of the standard replacement, the expansion of the elementary nucleon-nucleon amplitude f_j over the ratio $|\mathbf{Q}_j|/|\mathbf{p}|$. We will use the simple standard replacement in writing the formulas, for the sake of simplicity, but will allow for the possibility of their modification.

Now we can integrate over $\mathbf{Q}_j$ which leads to

$$B_{fi}^{(2)}=\frac{-(2\pi)^4}{(2\pi i p_0)^2}\left\langle f\left|\sum_{1=j<k}^{4} f_j\left(\frac{\mathbf{p}}{2}\right)f_k\left(\frac{\mathbf{p}}{2}\right)\delta(\boldsymbol{\rho}_k-\boldsymbol{\rho}_j)\right.\right.$$
$$\left.\left.\times\exp\left[i\mathbf{p}\cdot\left(\frac{\boldsymbol{\rho}_j+\boldsymbol{\rho}_k}{2}-\mathbf{R}_b\right)\right]\right|i\right\rangle. \tag{19}$$

For the wave function of the virtually excited cluster we can again use the fractional parentage expansion, but now with the two-particle fpc. They may be calculated by analogy with one-particle ones, see Appendix A. Table IV contains all two-particle fpc's needed for our purpose. The transformation to the set of the cluster Jacobi coordinates reads in this case

$$\mathbf{x}=\boldsymbol{\rho}_k-\boldsymbol{\rho}_j$$

and

$$\frac{\mathbf{X}}{2}=-\frac{\boldsymbol{\rho}_j+\boldsymbol{\rho}_k}{2}-\mathbf{R}_b,$$

where $\mathbf{x}$ is the intrinsic Jacobi coordinate of a two-nucleon system and $\mathbf{X}$ is the relative motion coordinate of two-nucleon pairs.

After rather routine work one can find

$$B_{fi}^{(2)} = -6 \frac{(2\pi)^4}{(2\pi i p_0)^2} \sum_{S_2,T_2,n_2,l_2,N_3,L_3,T_3} \langle 4[4]N_0L_00T_0|2[2]00S_2T_2;n_2l_2,2[2]N_3L_3S_2T_3\{L_0\}\rangle$$

$$\times \langle 4[4]0000|2[2]00S_2T_2;00,2[2]00S_2T_2\{0\}\rangle \sum_{M_{T_3},M_{T_2}} (T_2M_{T_2},T_3M_{T_3}|T_0M_{T_0})(-1)^{T_2-M_{T_2}}\frac{1}{\sqrt{2T_2+1}}$$

$$\times \sum_{m_{l_2},M_{L_3}} (L_3M_{L_3},l_2,m_{l_2}|L_0M_{L_0})\left[\frac{1}{4\pi}\right]^{1/2} Y_{l_2m_{l_2}}(\hat{\mathbf{p}})I_{n_2l_2}(p/2)\left\langle T_2-M_{T_2}\left|f_j\left(\frac{\mathbf{p}}{2}\right)f_k\left(\frac{\mathbf{p}}{2}\right)\right|T_3M_{T_3}\right\rangle$$

$$\times \langle 000|\delta(\mathbf{x})N_3L_3M_{L_3}\rangle. \tag{20}$$

Further simplifications result from the fact that $\mathbf{x}$ is a two-dimensional vector which lies in the plane perpendicular to the proton direction. The transformation matrix $C(nlm;n_0mn_z)$ from spherical wave functions to cylindrical ones, which is necessary for calculating $\langle 000|\delta(\mathbf{x})|N_3L_3M_{L_3}\rangle$, is derived in Appendix B, and the values of the matrix elements are placed in Table V.

After lengthy calculations one may obtain an expression for the deexcitation amplitudes of the second multiplicity

$$B^{(2)} = \frac{12(\pi)^{1/2}}{(p_0x_0)^2} \sum_{n_2,l_2,N_3,L_3} Y_{l_2M_{L_0}}(\hat{\mathbf{p}})C(N_3L_30;N_300)(L_30,l_2M_{L_0}|L_0M_{L_0})I_{n_2l_2}(p/2)$$

$$\times\left(\frac{(f_{pp}+f_{pn})^2}{4}\langle 4[4]N_0L_000|2[2]0010;n_2l_2,2[2]N_3L_310\{L_0\}\rangle\langle 4[4]0000|2[2]0010;00,2[2]0010\{0\}\rangle\right.$$

$$\left.+\frac{f_{pp}^2+f_{pn}^2}{6}\langle 4[4]N_0L_000|2[2]0001;n_2l_22[2]N_3L_301\{L_0\}\rangle\langle 4[4]0000|2[2]0001;00,2[2]0001\{0\}\rangle\right). \tag{21}$$

Now it is possible to evaluate the relative contribution of the processes of first and second multiplicities. A rough estimation of the ratio $\gamma_{21}=B_{fi}^{(2)}/B_{fi}^{(1)}$ gives the following result: the estimated ratio depends upon the value $f(\mathbf{p})/p_0$; in real experimental conditions (at fixed initial kinetic energy of the incident proton of 296 MeV, and at relatively small momentum transfer 460–475 MeV/c) γ_{21} does not exceed 1%. The same is approximately true for all consecutive ratios $\gamma_{n+1,n}$. Therefore it is possible to exclude from the further consideration all scattering multiplicities higher than the first one. In this case the theoretical treatment is greatly simplified.

E. The first multiplicity amplitude in the PWIA

Here we present the final expressions for the Glauber transition amplitudes taking into account only processes of the first multiplicity. In this case one can sum explicitly over all angular-momentum projections and obtain the result in terms of the Legendre polynomials of the angle between the momentum transfer and the recoil momentum of the residual nucleus. If the residual ^{8}Be nucleus is detected in its ground state, we immediately find

$$g_{fi} = \frac{f_{pp}+f_{pn}}{2\sqrt{\pi}}\sum_{\{[f],L,L\}}a_{[f],L,L}^{12,00}\sum_{\{[f_1],L_1,L\}}a_{[f_1],L_1,L}^{8,00}$$

$$\times\sum_{N_0,L_0}\langle 12[f]8LL0|8[f_1]4L_1L0;$$

$$4-N_0L_0,4[4]N_0L_000\{0\}\rangle(-1)^{L+L_1}$$

$$\times(-i)^{L_0}\sqrt{2L_0+1}\left\langle 4[4]N_0L_000\left|3[3]00\frac{1}{2}\frac{1}{2},N_0L_0\right.\right\rangle$$

$$\times P_{L_0}(\cos(\widehat{\mathbf{q},\mathbf{p}}))I_{N_0L_0}(3p/4)\int_0^\infty R^2j_{L_0}(qR)$$

$$\times R_{4-N_0L_0}(R)dR. \tag{22}$$

Table VI collects the α-particle fpc in the TISM.

TABLE V. The elements of the transition matrix from spherical to cylindrical coordinates.

N_3	L_3	$C(N_3L_30;N_300)$
0	0	1
2	0	$\sqrt{\frac{2}{3}}$
2	2	$\frac{1}{\sqrt{3}}$
4	0	$\sqrt{\frac{8}{15}}$
4	2	$\sqrt{\frac{8}{21}}$
4	4	$\sqrt{\frac{3}{35}}$

TABLE VI. The α-particle fpc in the TISM.

[f]	L	[f₁]	L₁	ℒ	N₀	L₀	Λ	Coefficient	[f]	L	[f₁]	L₁	ℒ	N₀	L₀	Λ	Coefficient
[44]	0	[4]	0	0	0	0	0	$\dfrac{-\sqrt{3}}{10\sqrt{22}}$	[431]	1	[31]	1	2	3	3	1	$\dfrac{-\sqrt{7}}{15\sqrt{110}}$
[44]	0	[4]	0	0	2	0	0	$\dfrac{-1}{3\sqrt{165}}$	[431]	1	[31]	1	2	4	2	0	$\dfrac{\sqrt{7}}{6\sqrt{165}}$
[44]	0	[4]	0	0	2	2	2	$\dfrac{-2}{15\sqrt{33}}$	[431]	1	[31]	3	2	0	0	2	$\dfrac{-3\sqrt{3}}{80\sqrt{22}}$
[44]	0	[4]	0	0	3	1	1	$\dfrac{2\sqrt{2}}{15\sqrt{33}}$	[431]	1	[31]	3	2	2	0	2	$\dfrac{-\sqrt{7}}{40\sqrt{66}}$
[44]	0	[4]	0	0	4	0	0	$\dfrac{-\sqrt{2}}{3\sqrt{165}}$	[431]	1	[31]	3	2	2	2	0	$\dfrac{-\sqrt{7}}{40\sqrt{66}}$
[44]	0	[4]	2	2	0	0	2	$\dfrac{\sqrt{3}}{4\sqrt{110}}$	[431]	1	[31]	3	2	2	2	2	$\dfrac{-1}{20\sqrt{66}}$
[44]	0	[4]	2	2	2	0	2	$\dfrac{\sqrt{7}}{6\sqrt{330}}$	[431]	1	[31]	3	2	3	1	1	$\dfrac{\sqrt{7}}{20\sqrt{165}}$
[44]	0	[4]	2	2	2	2	0	$\dfrac{\sqrt{7}}{6\sqrt{330}}$	[431]	1	[31]	3	2	3	3	1	$\dfrac{1}{20\sqrt{55}}$
[44]	0	[4]	2	2	2	2	2	$\dfrac{1}{3\sqrt{330}}$	[431]	1	[31]	3	2	4	2	0	$\dfrac{-1}{4\sqrt{330}}$
[44]	0	[4]	2	2	3	1	1	$\dfrac{-\sqrt{7}}{15\sqrt{33}}$	[431]	1	[31]	3	4	0	0	4	$\dfrac{-9}{80\sqrt{11}}$
[44]	0	[4]	2	2	3	3	1	$\dfrac{-1}{15\sqrt{11}}$	[431]	1	[31]	3	4	4	4	0	$\dfrac{-1}{4\sqrt{55}}$
[44]	0	[4]	2	2	4	2	0	$\dfrac{1}{3\sqrt{66}}$	[431]	1	[31]	3	4	2	2	2	$\dfrac{3}{20\sqrt{22}}$
[431]	1	[31]	1	0	0	0	0	$\dfrac{\sqrt{3}}{20\sqrt{22}}$	[431]	1	[31]	3	4	3	3	1	$\dfrac{1}{10\sqrt{11}}$
[431]	1	[31]	1	0	2	0	0	$\dfrac{1}{6\sqrt{165}}$	[422]	0	[22]	0	0	0	0	0	$\dfrac{-\sqrt{3}}{16\sqrt{22}}$
[431]	1	[31]	1	0	2	2	2	$\dfrac{1}{15\sqrt{33}}$	[422]	0	[22]	0	0	2	0	0	$\dfrac{-\sqrt{5}}{24\sqrt{33}}$
[431]	1	[31]	1	0	3	1	1	$\dfrac{\sqrt{2}}{15\sqrt{33}}$	[422]	0	[22]	0	0	2	2	2	$\dfrac{-1}{12\sqrt{33}}$
[431]	1	[31]	1	0	4	0	0	$\dfrac{1}{3\sqrt{330}}$	[422]	0	[22]	0	0	3	1	1	$\dfrac{1}{6\sqrt{66}}$
[431]	1	[31]	1	2	0	0	2	$\dfrac{\sqrt{21}}{40\sqrt{11}}$	[422]	0	[22]	0	0	4	0	0	$\dfrac{-\sqrt{5}}{12\sqrt{66}}$
[431]	1	[31]	1	2	2	0	2	$\dfrac{7}{60\sqrt{33}}$	[422]	2	[22]	2	0	0	0	0	$\dfrac{-\sqrt{3}}{40\sqrt{22}}$
[431]	1	[31]	1	2	2	2	0	$\dfrac{7}{60\sqrt{33}}$	[422]	2	[22]	2	0	2	0	0	$\dfrac{-1}{12\sqrt{165}}$
[431]	1	[31]	1	2	2	2	2	$\dfrac{\sqrt{7}}{30\sqrt{33}}$	[422]	2	[22]	2	0	2	2	2	$\dfrac{-1}{30\sqrt{33}}$
[431]	1	[31]	1	2	3	1	1	$\dfrac{-7}{15\sqrt{330}}$	[422]	2	[22]	2	0	3	1	1	$\dfrac{1}{15\sqrt{66}}$

TABLE VI. *(Continued).*

$[f]$	L	$[f_1]$	L_1	$\mathcal{L}$	N_0	L_0	Λ	Coefficient	$[f]$	L	$[f_1]$	L_1	$\mathcal{L}$	N_0	L_0	Λ	Coefficient
[422]	2	[22]	2	0	4	0	0	$\dfrac{-1}{6\sqrt{330}}$	[422]	2	[22]	2	4	2	2	2	$\dfrac{-3\sqrt{3}}{40\sqrt{11}}$
[422]	2	[22]	2	2	0	0	2	$\dfrac{-\sqrt{3}}{16\sqrt{55}}$	[422]	2	[22]	2	4	3	3	1	$\dfrac{-\sqrt{3}}{10\sqrt{22}}$
[422]	2	[22]	2	2	2	0	2	$\dfrac{-\sqrt{7}}{24\sqrt{165}}$	[422]	2	[22]	0	2	0	0	2	$\dfrac{-\sqrt{21}}{32\sqrt{55}}$
[422]	2	[22]	2	2	2	2	0	$\dfrac{-\sqrt{7}}{24\sqrt{165}}$	[422]	2	[22]	0	2	2	0	2	$\dfrac{-7}{48\sqrt{165}}$
[422]	2	[22]	2	2	2	2	2	$\dfrac{-1}{12\sqrt{165}}$	[422]	2	[22]	0	2	2	2	0	$\dfrac{-7}{48\sqrt{165}}$
[422]	2	[22]	2	2	3	1	1	$\dfrac{\sqrt{7}}{30\sqrt{66}}$	[422]	2	[22]	0	2	2	2	2	$\dfrac{-\sqrt{7}}{24\sqrt{165}}$
[422]	2	[22]	2	2	3	3	1	$\dfrac{1}{30\sqrt{22}}$	[422]	2	[22]	0	2	3	1	1	$\dfrac{7}{60\sqrt{66}}$
[422]	2	[22]	2	2	4	2	0	$\dfrac{1}{12\sqrt{33}}$	[422]	2	[22]	0	2	3	3	1	$\dfrac{\sqrt{7}}{60\sqrt{22}}$
[422]	2	[22]	2	4	0	0	4	$\dfrac{-9\sqrt{3}}{80\sqrt{22}}$	[422]	2	[22]	0	2	4	2	0	$\dfrac{-\sqrt{7}}{24\sqrt{33}}$
[422]	2	[22]	2	4	4	4	0	$\dfrac{\sqrt{3}}{4\sqrt{110}}$									

For the transition accompanied by the excitation of the lowest excited level 2^+ of the residual ^{8}Be nucleus we have a more complicated expression:

$$g_{fi}=\frac{2\sqrt{\pi}}{\sqrt{5}}(f_{pp}+f_{pn})\sum_{\{[f],L,L\}}a^{12,00}_{[f],L,L}\sum_{\{[f_1],L_1,L\}}a^{8,00}_{[f_1],L_1,L}\sum_{N_0,L_0,\Lambda}\langle 12[f]8LL0|8[f_1]4L_1L0;4-N_0\Lambda,4[4]N_0L_000\{2\}\rangle$$

$$\times(-1)^{L+L_1}i^{\Lambda}\left\langle 4[4]N_0L_000\Big|3[3]00\frac{1}{2}\frac{1}{2},N_0L_0\right\rangle I_{N_0L_0}(3p/4)\int_0^{\infty}R^2 j_{\Lambda}(qR)R_{4-N_0\Lambda}(R)dR$$

$$\times\sum_{M_{L_0},M_\Lambda}(-1)^{M_2}(\Lambda M_\Lambda,L_0 M_{L_0}|2-M_2)Y_{\Lambda M_\Lambda}(\hat{\mathbf{q}})Y_{L_0 M_{L_0}}(\hat{\mathbf{p}}). \qquad (23)$$

Here M_2 is the projection of the final angular momenta of the ^{8}Be nucleus. This expression may be transformed into a more suitable one, taking into account that the cross section depends upon the square of the absolute value of g_{fi}.

F. The first multiplicity amplitude in the DWIA

Direct comparison of the PWIA calculations with the experimental data is not quite reasonable, due to the large absorption under experimental conditions. For the reasons dis-

cussed in the Introduction one needs to account for the distortions. For the sake of simplicity, we consider here only the distortions in the final state due to the α-^{8}Be interaction. This seems reasonable keeping in mind the relatively low energy of α-^{8}Be mutual motion (about 20 MeV near the quasielastic peak). The interaction between the initial proton and the ^{12}C nucleus, as well as between the scattered proton and the residual ^{8}Be nucleus, may be taken into account in the same way. Because of the higher energy of relative mo-
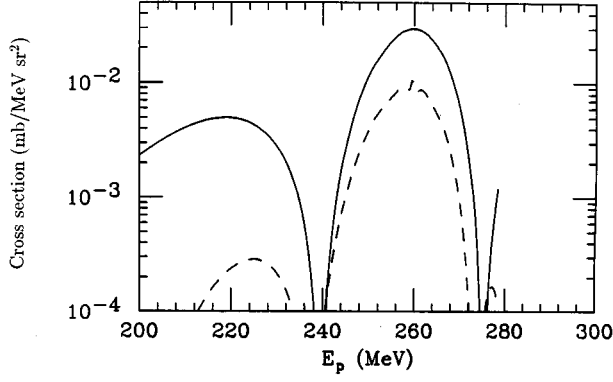
FIG. 4. The triple-differential cross section of the ^{12}C$(p,p'\alpha)^8$Be reaction at $\theta_p = 35°$ calculated in the PWIA. The dashed line shows the contribution of the diagonal, with respect to the states of the knockedout α cluster, transitions. The solid line corresponds to all possible transitions from virtually excited states of the α cluster inside the target nucleus.

tion in those last pairs compared to the α-^{8}Be pair, we neglect these distortions in the first approximation.

We will consider distortions in the framework of the usual DWIA procedure by introducing the optical potentials, with their real and imaginary parts, and solving the corresponding two-body Schrödinger equations. We postpone the discussion of which optical potentials were used until the next section.

The wave function of the final state in this case may be written, instead of Eq. (7), as

$$\Psi_f^{(-)} = \exp[i(\mathbf{p}_\alpha - \mathbf{q}) \cdot \mathbf{R}_A]\hat{\mathcal{A}}$$
$$\times [\chi^{(-)}(\mathbf{k},\mathbf{R})\Psi_f^{A-b}|4[4]0000:000\rangle]. \quad (24)$$

Here $\mathbf{k}$ is the momentum of relative motion of the emitted α cluster and the residual ^{8}Be nucleus, $\mathbf{R}_A$ is the center-of-mass vector of the target nucleus.

The distorted wave $\chi^{(-)}(\mathbf{k},\mathbf{R})$ may be expressed as the partial-wave expansion,

$$\chi^{(-)*}(\mathbf{k},\mathbf{R}) = 4\pi\sum_{l=0}^{\infty}\sum_{m_l=-l}^{l}(-i)^l\chi_l^*(k,R)$$
$$\times [Y_{lm_l}(\hat{\mathbf{R}})]^*Y_{lm_l}(\hat{\mathbf{k}}). \quad (25)$$

Using standard geometrical transformations one can obtain the final expression for the Glauber transition amplitude. We write it only for the transition to the ground state of the residual nucleus, because the difference between this transition and transitions to the excited states of ^{8}Be is merely technical:

$$g_{fi} = \sqrt{\frac{55}{\pi}}(f_{pp}+f_{pn})\sum_{\{[f],L,L\}}a_{[f],L,L}^{12,00}\sum_{\{[f_1],L-1,L\}}a_{[f_1],L_1,L}^{8,00}\sum_{N_0,L_0}\langle 12[f]8LL0|8[f_1]4L_1L0;$$

$$4-N_0L_0,4[4]N_0L_000\{0\}\rangle(-1)^{L_1+L}\left\langle 4[4]N_0L_000\left|3[3]\frac{1}{2}\frac{1}{2},N_0L_0\right\rangle I_{N_0L_0}(3p/4)\right.$$

$$\times\sum_{l,l_1=0}^{\infty}(-i)^{l+l_1}(-1)^{-l}(2l_1+1)\sqrt{2l+1}(L_00,l_10|l0)(l_10,l0|L_00)$$

$$\times P_l[\cos(\widehat{\mathbf{k},\mathbf{p}})]\int_0^{\infty}R^2j_{l_1}\left(\frac{2}{3}pR\right)\chi_l^*(k,R)R_{4-N_0L_0}(R)dR. \quad (26)$$

The argument of the Bessel function in the last line is due to the relative motion part of $\exp(-\frac{2}{3}i\mathbf{p}\cdot\mathbf{r})$.

III. RESULTS AND DISCUSSION

Now we discuss the possibility of observing evidence of virtually excited clusters in the quasielastic knockout experiments. We restrict ourselves to the typical reaction of this class ^{12}C$(p,p'\alpha)^8$Be. It is reasonable to expect that for other quasielastic knockout reactions ^{9}Be$(p,p'\alpha)^5$He, ^{7}Li$(p,p'\alpha)^3$H, and ^{6}Li$(p,p'\alpha)^2$H the situation does not change dramatically.

First of all we examine this reaction in the framework of the Glauber PWIA approximation. The reasons for this are (i) the PWIA approach is simple and transparent, so one can hope that the effects of nuclear structure can be more clearly

seen; (ii) the optical potentials used in the DWIA to account for distortions have various uncertainties which obscure the treatment; (iii) it is known that the main qualitative features of the energy dependence of the cross section (but not the absolute normalization) can be sufficiently well reproduced in the PWIA scheme [4].

Figure 4 shows the triple differential cross section of the reaction as a function of the scattered proton energy for $\theta_p = 35°$. The actual calculations were carried out with the parametrization of the elementary nucleon-nucleon amplitude taken from [30],

$$f(\mathbf{p}) = \frac{p_0\sigma}{4\pi}[i\exp(-\beta^2p^2/2)+\xi\exp(-\beta'^2p^2/2)], \quad (27)$$

TABLE VII. The parametrization of the elementary nucleon-nucleon amplitudes.

p-N	σ (mb)	β^2 $(GeV/c)^{-2}$	β'^2 $(GeV/c)^{-2}$	ξ
p-p	25.0	13.6	24.2	1.22
p-n	47.7	17.9	25.0	0.84

with the values of the parameters indicated in Table VII. The maximum of the cross section is situated precisely in the quasifree scattering region where the momentum of the residual ^{8}Be nucleus vanishes. The contribution from the diagonal transition with respect to the states of the emitted α cluster is shown by the dashed line. This part is determined mainly by the two largest components of the wave function of target ^{12}C and residual ^{8}Be nuclei with quantum numbers $[f]=[44]$, $[f_1]=[4]$, $L=L_1=S=S_1=0$ and $[f]=[431]$, $[f_1]=[31]$, $L=L_1=S=S_1=1$, respectively. The other components are substantially smaller and they manifest themselves mainly through the interference with the main components. The full contribution from all possible transitions is shown by the solid line. In this case a number of possible transitions are determined by a number of possible α cluster states inside the target nucleus. The knocked out α cluster may possess the following sets of quantum numbers in the standard shell-model scheme: (1) $N_0=0$, $L_0=0$, usual α particle ground state; (2) $N_0=2$, $L_0=0$; (3) $N_0=2$, $L_0=2$; (4) $N_0=3$, $L_0=1$; (5) $N_0=3$, $L_0=3$; (6) $N_0=4$, $L_0=0$; (7) $N_0=4$, $L_0=2$; and (8) $N_0=4$, $L_0=4$. Taking into account this classification and the shell-model structure of the wave functions (Tables I and II) one can easily find the number of permissible transitions.

We do not consider here possible α-cluster states with spin-isospin excitations because the lowest states of the residual nucleus automatically select the cluster states without such excitation. But this conclusion is valid only for cross sections summed over all spin projections. An experiment with polarized protons is, in principle, capable of probing spin-isospin excitations as well if the final polarization characteristics are measured. In this case one needs to explicitly introduce the spin-isospin dependence of the elementary nucleon-nucleon amplitudes. The situation is similar and complementary to that in the electron knockout experiment [29].

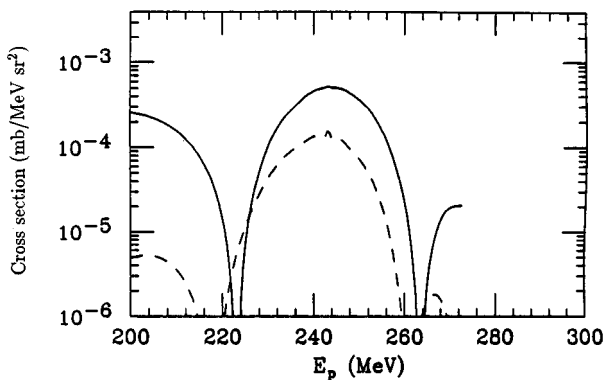Each of the nondiagonal transitions by itself is rather
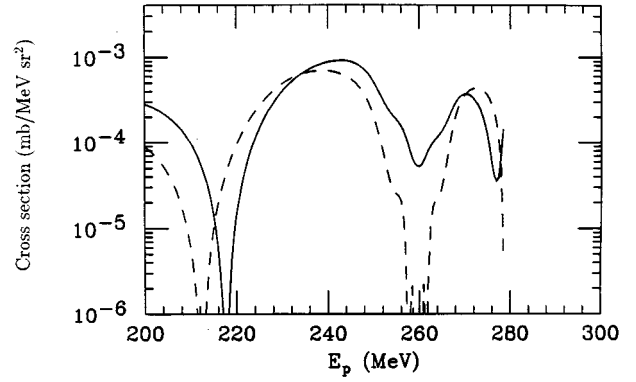

FIG. 6. The same as Fig. 4 but for the transition into the first excited 2^+ state of the residual nucleus.

weak, but the combined contribution via their interference with diagonal counterparts becomes noticeable. The ratio of the values between the two curves in the region of quasifree scattering reaches 2. This demonstrates the importance of the effect of virtually excited clusters and makes a more accurate treatment desirable. Remember that we use a rather rough Glauber approach, which is based on an empirical parametrization of elementary nucleon-nucleon amplitudes [30] for high energies and small scattering angles, at relatively small energies and scattering angles which are too large for this approach. Therefore our results can be considered as a first evidence only.

Figure 5 shows the same cross section as Fig. 4 but for another proton scattering angle, $\theta_p=45°$. We obtain qualitatively the same picture as earlier but with a significantly lowered magnitude. This may be a consequence of the parametrization of elementary nucleon-nucleon amplitudes, Eq. (27), which is hardly justified at scattering angles too large for the Glauber approach.

Figure 6 shows the knockout reaction cross section at the same kinematic conditions as Fig. 4 but for the events when the residual nucleus appears in the lowest excited state 2^+ with excitation energy 2.9 MeV. It is expected that the cross section for such events is much lower than that for the transition to the ground state. Figure 7 is analogous to Fig. 6 but demonstrates the cross section for $\theta_p=45°$. The ratio of the maxima of the cross sections corresponding to transitions to the excited and ground state of ^{8}Be does not exceed 3%.
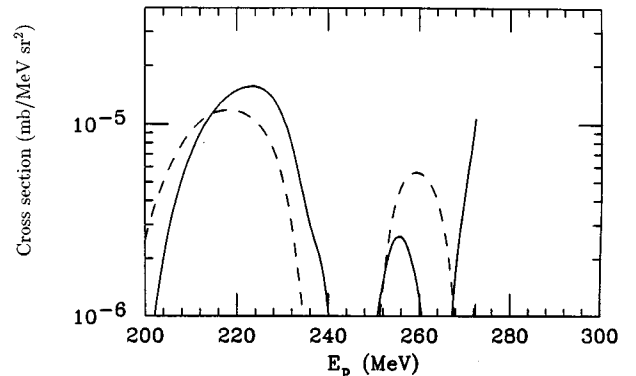

FIG. 5. The same as Fig. 4 but for $\theta_p=45°$.

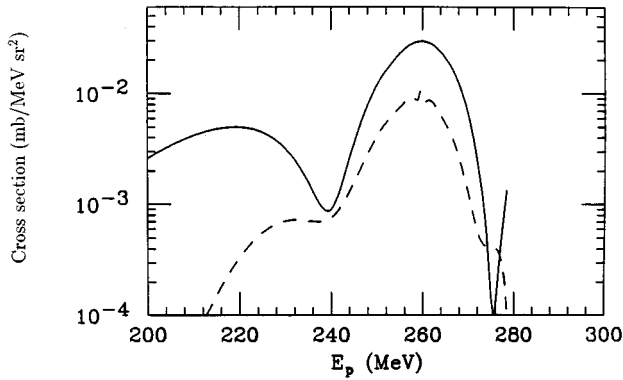FIG. 7. The same as Fig. 6 but for $\theta_p=45°$.

FIG. 8. The sum of the cross sections, depicted in Figs. 4 and 6.

This is important because, if the final states of the residual nucleus are not experimentally resolved, one needs to know the relative fraction of different transitions.

In Figs. 8 and 9, the integral cross sections for two different proton scattering angles are shown. They are the sums of the cross sections for the transitions to the ground and first excited states of the residual nucleus. The notations are the same as in previous figures.

Finally, in Figs. 10 and 11, again for $\theta_p = 35°$ and $45°$, respectively, we present the calculations of the quasielastic knockout cross section taking into account the final-state interaction between the emitted α particle and the residual ^{8}Be nucleus. Here we have taken into account only the transition into the ground state of the residual nucleus. We see the essential distortion effects in the redistribution of the reaction strength. The quasielastic peak is much more pronounced as compared to the secondary maxima. It is more narrow and slightly shifted to high energies. The comparison with the PWIA calculations, Figs. 4 and 5, shows that the main result of distortion is revealed through the interference of different excitation amplitudes which turns out to be destructive in the region of the secondary peak. In the region of energies below the quasifree peak, the excited cluster configurations in the target increase the observed cross section by order of magnitude.

The shortcoming of the whole approach is associated with the lack of information concerning the final-state optical potential. In the calculation we used the optical potential taken from [10] and corrected according to the standard prescriptions: the strength of the real part of the optical-model po-
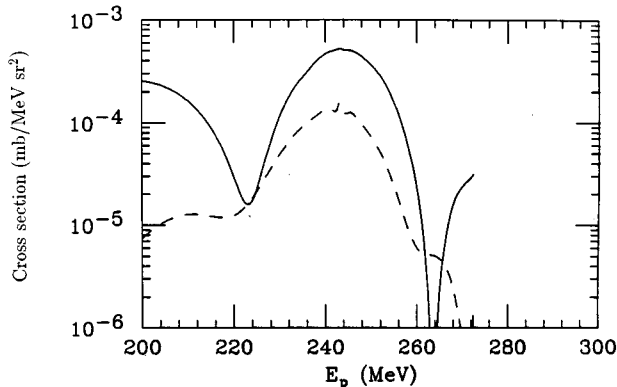

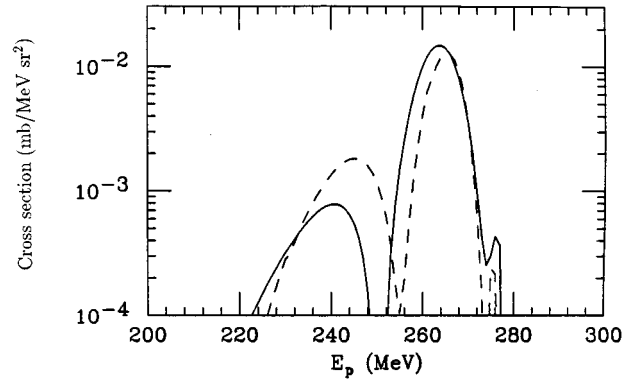FIG. 10. The results of DWIA calculations for the transition into the ground state of the ^{8}Be nucleus and $\theta_p = 35°$. The notations are the same as in Fig. 4.

tential decreases logarithmically with energy [31,32] and the imaginary part slightly increases [33]. Instead of the value -89.9 MeV for the real part of the optical potential [10] we have introduced the energy dependence in the form of $V_0(E) = V_0(1 - \eta \ln E)$ and selected the value of the parameter $\eta = 0.035$ if energy is measured in MeV. The strength of the imaginary part of the optical potential in the region of the quasifree peak was nearly -2.5 MeV. Unfortunately, there exists no justified optical model potential for the α-^{8}Be system; the use of the corrected α-^{9}Be potential [10] implies unknown uncertainties because the structure of the two Be isotopes is very different.

IV. CONCLUSIONS

We performed calculations for the quasielastic knockout of the alpha cluster from the typical shell-model nucleus ^{12}C. Our major interest was focused on the nuclear structure questions related to the problem of the existence of excited cluster configurations. Relevant spectroscopic information cannot be extracted without a reasonable description of the reaction mechanism. The usual theoretical approaches, such as the Glauber method, have their limitations, especially for not very high energies and relatively large scattering angles. The lack of information concerning the optical potential between the emitted cluster and the residual nucleus is another source of uncertainties. Nevertheless some preliminary con-
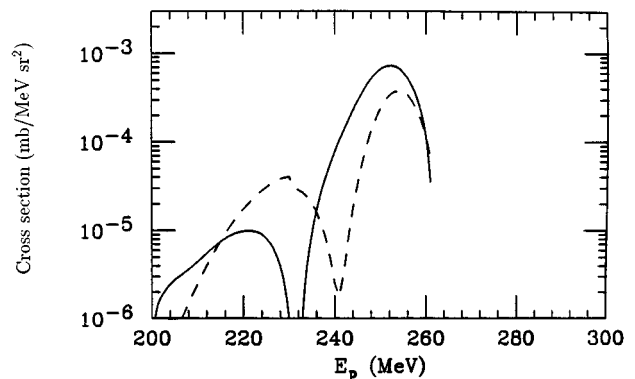

FIG. 9. The sum of the cross sections, depicted in Figs. 5 and 7.

FIG. 11. The results of DWIA calculations for the transition into the ground state of the ^{8}Be nucleus and $\theta_p = 45°$. The notations are the same as in Fig. 5.

clusions can be drawn already at this stage.

The traces of virtually excited clusters are present even at relatively small scattering energies.

The contribution of deexcitation amplitudes in a total reaction cross section, taking into account all virtual channels and their interference, strongly depends upon momentum transfer and energy of the incident particle. At sufficiently large energies when the different scattering multiplicities are getting more important, the effects of virtually excited clusters are expected to be more pronounced and apparently more observable due to the interplay of a greater number of harmonics associated with different permissible states of the emitted cluster.

In the energy sharing experiments the difference between diagonal and nondiagonal (with respect to the states of the emitted cluster) transitions and therefore cross sections is mainly quantitative. An angular distribution experiment seems to be more efficient to display the signatures of the virtual cluster states. It is possible to chose such kinematical conditions that the deexcitation amplitudes may have maximum values when the diagonal ones have minimum values.

It is reasonable to look for the presence of virtually excited nucleon configurations in polarization experiments. The electron-scattering experiments made in parallel would be very useful to clarify the situation.

The contribution of the first excited state of the residual nucleus, ^{8}Be in the considered case, is suppressed at not very high energies compared to the contribution of the ground state. This can be useful for the interpretation of experiments with limited resolution.

APPENDIX A: ONE-PARTICLE FRACTIONAL PARENTAGE COEFFICIENTS IN TISM

We need the following one-particle fractional parentage coefficients for the calculation of first scattering multiplicity deexcitation amplitudes:

$$A_{NL} = \left\langle 4[4]NL00 \middle| 3[3]00\frac{1}{2}\frac{1}{2},NL \right\rangle.$$

These fpcs describe the separation of a nucleon from a fully symmetric spatial four-nucleon configuration with the antisymmetric spin-isospin part of the wave function. The number of oscillator quanta N and total orbital momentum L of

the four-nucleon configuration are arbitrary and compatible with the Young scheme $[f]=[4]$, irrespective of the shell to which the nucleons belong.

In our calculations we use the general prescription for the computation of the fpc in the TISM given in [34]. The method is a modification for the TISM of Redmond's formula [35].

Since $[3] \times [1] = [4] + [31]$, we can choose

$$\left| 3[3]00\frac{1}{2}\frac{1}{2},NL:L00 \right\rangle$$

as a parental state. In this case we automatically obtain a correct result due to incompatibility of spatial symmetry [31] and spin-isospin quantum numbers $S=0$, $T=0$. Operating on the parental state with the antisymmetrization operator, we obtain

$$|4[4]NL00\rangle = \frac{1}{Q}\left\{ 1 - \sum_{i=1}^{3} P_{i4} \right\} \times \left| 3[3]00\frac{1}{2}\frac{1}{2},NL:L00 \right\rangle,$$

where P_{i4} is the permutation operator and Q is the normalization factor.

Denoting for brevity

$$\Pi_{NL} \equiv \left\langle 3[3]00\frac{1}{2}\frac{1}{2},NL:L00 \middle| P_{3,4} \middle| 3[3]00\frac{1}{2}\frac{1}{2},NL:L00 \right\rangle,$$

we obtain

$$A_{NL} = \frac{\sqrt{1-3\Pi_{NL}}}{2}.$$

Now we can calculate the matrix element of the permutation operator P_{34} using again the one-particle fpc but for the three-nucleon system. We can separate the third nucleon in the left and right sides of the matrix element. Then we must transform to the new set of Jacobi coordinates with the help of Talmi-Moshinsky-Smirnov coefficients and change the order of momenta coupling. In this case

$$\Pi_{NL} = \sum_{S,T,\mathcal{L}} \left\langle 3[3]00\frac{1}{2}\frac{1}{2} \middle| 2[2]00ST,00 \right\rangle$$

$$\times \left\langle 3[3]00\frac{1}{2}\frac{1}{2} \middle| 2[2]00ST,00 \right\rangle$$

$$\times W\left(\frac{1}{2}S0\frac{1}{2};\frac{1}{2}\frac{1}{2}\right) W\left(\frac{1}{2}T0\frac{1}{2};\frac{1}{2}\frac{1}{2}\right)$$

$$\times W(00LL;0\mathcal{L}) W(00LL;0\mathcal{L})$$

$$\times (-1)^{S+T+L}\langle NL,00:\mathcal{L}|1/8|NL,00:\mathcal{L}\rangle$$

$$= \sum_{S,T} \left\langle 3[3]00\frac{1}{2}\frac{1}{2} \middle| 2[2]00ST,00 \right\rangle^2 (-1)^{S+T+L}$$

$$\times \langle NL,00:L|1/8|NL,00:L\rangle.$$

Here the $\langle NL,00:L|1/8|NL,00:L\rangle$ is a usual Talmi-Moshinsky-Smirnov coefficient equal in our case to $(1/9)^{N/2}$.

Taking into account that for the one-particle fpc we always have factorization into orbital and spin-isospin parts and using the particular values of spin-isospin fpc and the standard notations [14], we obtain

$$\left\langle 3[3]00\frac{1}{2}\frac{1}{2}\Big|2[2]00ST,00\right\rangle$$

$$=\langle 3[3]0|2[2]0,1[1]0\rangle\left\langle (st)^3[\widetilde{3}]\frac{1}{2}\frac{1}{2}\Big|(st)^2[\widetilde{2}]ST\right\rangle$$

$$=\langle 3[3]0|2[2]0,1[1]0\rangle\left\langle (st)^3[\widetilde{3}]\frac{1}{2}\frac{1}{2}\Big|(st)^2[\widetilde{2}]ST\right\rangle$$

$$\times\begin{cases}\sqrt{\dfrac{1}{2}} & \text{if } T=0 \text{ and } S=1,\\[2mm] -\sqrt{\dfrac{1}{2}} & \text{if } T=1 \text{ and } S=0.\end{cases}$$

Therefore $\Pi_{NL}=(-1)^{L+1}3^{-N}$, and, finally

$$A_{NL}=\frac{1}{2}\sqrt{1-(-1)^{L+1}3^{1-N}}.$$

APPENDIX B: TRANSITION MATRIX TO CYLINDRICAL COORDINATES

In spherical coordinates the oscillator function is $\langle\mathbf{r}|nlm\rangle=R_{nl}(r)Y_{lm}(\theta,\varphi)$ where

$$R_{nl}(r)=\frac{2^{l/2+1}}{\pi^{1/4}r_0^{3/2}}\exp\left(-\frac{r^2}{2r_0^2}\right)\sum_{k=0}^{(n-l)/2}\frac{(-1)^k}{k!}r^{2k+l}$$

$$\times\frac{\sqrt{(n-l)!!(n+l+1)!!}}{(n-l-2k)!!(2l+2k+1)!!}.$$

Omitting the common exponential factor $\exp(-r^2/2r_0^2)$ and using the expansion of the spherical function in Cartesian coordinates, the leading term in powers of r is proportional to

$$\sum_{s=0}(-1)^s\frac{(2l-2s)!}{s!(l-s)!(l-m-2s)!}$$

$$\times(x+iy)^m z^{l-m-2s}r^{n-l+2s}.$$

Now one can use the binomial expansion

$$r^{n-l+2s}=\sum_{t=0}^{n-l+2s}\frac{[(n-l+2s)/2]!}{t![(n-l+2s)/2-t]!}\rho^{2t}z^{n-l+2s-2t}.$$

The main term in powers of z in the expansion of the one-dimensional oscillator function is $\sqrt{2^{n_z}/n_z!}\,z^{n_z}$. Comparing the powers of z, we have $n-m-2t=n_z$, and $t=(n-m-n_z)/2=(n_0-m)/2$ which eliminates the corresponding sum.

We repeat the same procedure for the two-dimensional remainder which is to be compared with the main term of the wave function in the two-dimensional polar coordinate frame. This gives the final result for the transformation matrix defined in Sec. II D,

$$C(nlm;n_0mn_z)$$

$$=2^{-(l+n_z)/2}(-1)^{(n_z-l)/2+2m}$$

$$\times\sqrt{\frac{(2l+1)(n-l)!!(l-m)!n_z![(1/2)(n_0+m)]!}{(n+l+1)!!(l+m)![(1/2)(n_0-m)]!}}$$

$$\times\frac{1}{[(n-l)/2]!}\sum_s(-1)^s$$

$$\times\frac{(2l-2s)![(n-l+2s)/2]!}{s!(l-s)!(l-m-2s)![(m-l+2s+n_z)/2]!}.$$

[1] G. Igo, L. E. Hansen, and T. G. Gooding, Phys. Rev. **131**, 337 (1963).

[2] A. N. James and H. G. Pugh, Nucl. Phys. **42**, 441 (1963).

[3] M. Riou, Rev. Mod. Phys. **37**, 375 (1965).

[4] B. Gottschalk and S. L. Kannenberg, Phys. Rev. C **2**, 24 (1970).

[5] V. V. Balashov, A. N. Boyarkina, and I. Rotter, Nucl. Phys. **A59**, 417 (1964).

[6] P. Beregi, N. S. Zelenskaya, V. G. Neudatchin, and Yu. F. Smirnov, Nucl. Phys. **A66**, 513 (1965).

[7] A. Nadasen, P. G. Roos, N. S. Chant, C. C. Chang, G. Ciangaru, H. F. Breuer, J. Wesick, and E. Norbeck, Phys. Rev. C **40**, 1130 (1989).

[8] G. R. Satchler, *Direct Nuclear Reactions* (Clarendon Press, Oxford, 1983).

[9] N. S. Chant and P. G. Roos, Phys. Rev. C **15**, 57 (1977).

[10] P. G. Roos, N. S. Chant, A. A. Cowley, D. A. Goldberg, H. D. Holmgren, and R. Woody, Phys. Rev. C **15**, 69 (1977).

[11] A. Nadasen, N. S. Chant, P. G. Roos, T. A. Carey, R. Cowen, C. Samanta, and J. Wesick, Phys. Rev. C **22**, 1394 (1980).

[12] T. A. Carey, P. G. Roos, N. S. Chant, A. Nadasen, and H. L. Chen, Phys. Rev. C **29**, 1273 (1984).

[13] C. W. Wang *et al.*, Phys. Rev. C **31**, 1662 (1985).

[14] V. G. Neudatchin, Yu. F. Smirnov, and N. F. Golovanova, Adv. Nucl. Phys. **11**, 1 (1979).

[15] V. G. Neudatchin, A. A. Sakharuk, W. W. Kurovsky, and Yu. M. Tchuvil'sky, Phys. Rev. C **50**, 148 (1994).

[16] Yu. M. Tchuvil'sky, W. W. Kurovsky, A. A. Sakharuk, and V. G. Neudatchin, Phys. Rev. C **51**, 784 (1995).

[17] R. G. Glauber, *Lectures in Theoretical Physics* (Interscience, New York, 1953), p. 315.

[18] G. D. Alkhazov, S. L. Belostotsky, and A. A. Vorobyov, Phys. Rep. **42**, 89 (1978).

[19] T. Yoshimura *et al.*, private communication.

[20] L. I. Schiff, Phys. Rev. **103**, 443 (1956).

[21] S. J. Wallace, Ann. Phys. (N.Y.) **78**, 190 (1973).

[22] S. J. Wallace, Phys. Rev. C **8**, 2043 (1973).

[23] J. Hüfner, Ann. Phys. (N.Y.) **115**, 43 (1978).

[24] A. C. Williams, Ann. Phys. (N.Y.) **129**, 22 (1980).

[25] K. M. Maung, J. Phys. G **20**, L99 (1994).

[26] C. J. Joachain, *Quantum Collision Theory* (North-Holland, Amsterdam, 1975).

[27] A. N. Boyarkina, *Structure of 1p-Shell Nuclei* (Moscow State University, Moscow, 1973).

[28] R. D. Lawson, *Theory of the Nuclear Shell Model* (Clarendon Press, Oxford, 1980).

[29] A. A. Sakharuk (unpublished).

[30] A. G. Sitenko, *Theory of Nuclear Reactions* (World Scientific, Singapore, 1990).

[31] A. Nadasen, P. Schwandt, P. P. Singh, W. W. Jacob, A. D. Bacher, P. T. Debevec, M. D. Kaitchuck, and J. T. Meek, Phys. Rev. C **23**, 1023 (1981).

[32] A. Nadasen, M. McMaster, M. Fingal, J. Tavormina, P. Schwandt, J. S. Winfield, M. F. Mohar, F. D. Becchetti, J. W. Jänecke, and R. E. Warner, Phys. Rev. C **39**, 536 (1989).

[33] A. Shridhar, N. Lingappa, S. K. Gupta, and S. Kailas, Phys. Rev. C **30**, 1760 (1984).

[34] I. V. Kurdyumov, Yu. F. Smirnov, K. V. Shitikova, and S. Kh. El Samarai, Nucl. Phys. **A145**, 593 (1970).

[35] P. J. Redmond, Proc. R. Soc. London Ser. A **222**, 84 (1954).